Materials Letters 253 (2019) 293–297

Contents lists available at ScienceDirect

Materials Letters

journal homepage: www.elsevier.com/locate/mlblue

Effects of $(Mg_{1/3}Nb_{2/3})$ substitution on the structure and microwave dielectric properties of Sr_2TiO_4 ceramics

Bing Liu [a,*], Cheng Chao Hu [b], Yu Hui Huang [c], Kai Xin Song [a,*]

[a] College of Electronic Information and Engineering, Hangzhou Dianzi University, Hangzhou 310018, China
[b] College of Materials Science and Engineering, Liaocheng University, Liaocheng 252059, China
[c] School of Materials Science and Engineering, Zhejiang University, Hangzhou 310027, China

ARTICLE INFO

Article history:
Received 11 June 2019
Received in revised form 28 June 2019
Accepted 1 July 2019
Available online 2 July 2019

Keywords:
Ceramics
Microstructure
Microwave dielectric properties

ABSTRACT

$Sr_2Ti_{1-x}(Mg_{1/3}Nb_{2/3})_xO_4$ ($0 \le x \le 0.4$) solid solutions were synthesized by standard solid-state reaction method for the first time, and their microwave dielectric properties were systematically investigated together with the microstructure. X-ray diffraction patterns revealed the formation of solid solutions in the whole composition range, while two kinds of secondary phases started to appear when $x = 0.4$. With increasing x, the dielectric constant (ε_r) was tuned from 42 to 26.3 and the temperature coefficient of resonant frequency (τ_f) could be successfully modified from 130 ppm/°C to 46.3 ppm/°C. Excellent combination of microwave dielectric properties with $\varepsilon_r = 28.5$, $Qf = 83{,}300$ GHz, and $\tau_f = 53$ ppm/°C were obtained for the $x = 0.3$ composition after sintering at 1500 °C for 3 h.

1. Introduction

Owing to the rapid development of wireless communication technology, microwave dielectric ceramics have been playing a key role in global society. Nowadays, the applications of microwave dielectric ceramics are all-pervasive, and the recent progress in the fifth generation wireless systems (5G), intelligent transport systems (ITS), Internet of Things (IoT) has resulted in an increasing demand for low-loss dielectric materials. In order to promote the development of the novel information technologies, it is a hot issue to search for new candidates with suitable dielectric constant (ε_r), high quality factor (Q) and near-zero temperature coefficient of resonant frequency (τ_f) [1].

In the past decades, Sr_2TiO_4 with layered Ruddlesden-Popper structure has been receiving increasing attention in the research community. Lee et al. reported that the Sr_2TiO_4 film exhibited stable chemical/physical properties and exceptionally low dielectric loss in the microwave frequency range [2]. For the bulk ceramics, our previous study has revealed the synthesis of Sr_2TiO_4 ceramics, and outstanding microwave dielectric properties were also obtained ($\varepsilon_r = 42$, $Qf = 145{,}000$ GHz, $\tau_f = 130$ ppm/°C) [3]. The good combination of ε_r and Qf value in Sr_2TiO_4 ceramics is superior to the typical low loss candidates such as $Ba[(Co,Zn)_{1/3}Nb_{2/3}]O_3$ ($\varepsilon_r = 34.5$, $Qf \sim 97{,}000$ GHz, $\tau_f \sim 0$ ppm/°C) [4]. However, the large positive τ_f value of Sr_2TiO_4 ceramics is barely satisfactory for practical application and should be further adjusted towards zero.

Generally, there are two common routes to adjust the τ_f, one is to form solid solutions and the other is to create composite ceramics. As the Qf value is very sensitive to the phase compositions and the formation of composite ceramics is usually deteriorating, the manner of creating solid solutions is preferred in this work. For titanate compounds, the substitution of $(Mg_{1/3}Nb_{2/3})^{4+}$ for Ti^{4+} has been widely confirmed to be effective in optimizing the τ_f values. Bian et al. have successfully tuned the τ_f value of Li_2TiO_3 ceramics to zero by forming $Li_2Ti_{1-x}(Mg_{1/3}Nb_{2/3})_xO_3$ solid solutions ($x = 0.24$) ($\varepsilon_r = 21$, $Qf = 200{,}000$ GHz, $\tau_f = -1$ ppm/°C) [5]. Similar modifications have been also achieved in many other material systems, such as $Ca[Ti_{0.35}(Mg_{1/3}Nb_{2/3})_{0.65}]O_3$ [6], $Ca_4La_2Ti_2(Mg_{1/3}Nb_{2/3})_3O_{17}$ [7], etc. However, to our best knowledge, no previous reports concerning the substitution of $(Mg_{1/3}Nb_{2/3})^{4+}$ in Sr_2TiO_4 ceramics have been reported. Motivated by this, it comes to be an important issue to understand the effects of $(Mg_{1/3}Nb_{2/3})^{4+}$ substitution on the microwave dielectric properties of Sr_2TiO_4 ceramics and this may trigger a new breakthrough in the application of high performance microwave dielectric ceramics.

In this work, $Sr_2Ti_{1-x}(Mg_{1/3}Nb_{2/3})_xO_4$ ceramics are prepared via a standard solid-state reaction method for the first time. The microwave dielectric properties are systematically investigated together with the evolution of phase compositions and microstructures.

* Corresponding authors.
E-mail addresses: liubing@hdu.edu.cn (B. Liu), kxsong@hdu.edu.cn (K.X. Song).

https://doi.org/10.1016/j.matlet.2019.07.002
0167-577X/

2. Experimental procedure

$Sr_2Ti_{1-x}(Mg_{1/3}Nb_{2/3})_xO_4$ (x = 0.1, 0.2, 0.3 and 0.4) ceramics were prepared via a solid-state reaction of $SrCO_3$ (99.95%), TiO_2 (99.99%), MgO (99.99%) and Nb_2O_5 (99.99%) powders. The stoichiometric powders were ball-milled in ethanol media and then calcined at 1250 °C in air for 3 h. After a second ball-milling, the powders were mixed with 4 wt% PVA solution and pressed into cylindrical pellets with 12 mm in diameter and 5 mm in height. The pellets were then sintered in the temperature range from 1475 °C to 1550 °C to obtain dense ceramics.

The relative density of the present ceramics was measured using the Archimedes method. The phase compositions of the sintered ceramics were determined using X-ray diffraction (XRD: D/max 2550/PC, Rigaku Co., Tokyo, Japan). Microstructures of the thermal etched surfaces were observed using scanning electron microscopy (SEM: S-3400, Hitachi, Tokyo, Japan). The microwave dielectric properties were evaluated using a network analyzer (E8363B, Agilent Technologies Inc., Santa Clara, CA). The evaluation of τ_f was carried out in the temperature range of 20 °C–80 °C.

3. Results and discussion

Fig. 1(a) shows the XRD patterns of $Sr_2Ti_{1-x}(Mg_{1/3}Nb_{2/3})_xO_4$ ceramics sintered at their optimal temperature. All the diffraction patterns in the compositions of $x \leq 0.3$ can be successfully indexed according to Sr_2TiO_4 (JCPDS #39-1471) and the relevant indices of crystallographic planes have been labeled. While, for x = 0.4, two kinds of secondary phases which could be matched as $Ti_2Nb_{10}O_{29}$ and $Mg_{1.05}Ti_{1.95}O_5$ co-exist with the main diffraction phase. For the present ceramics with layered perovskite structure, the structural stability is closely related with the size adaptability between perovskite and rock-salt layers, which is usually discussed in terms of the tolerance factor (t) [8]. Therefore, it is inferred that the appearance of secondary phases should be mainly ascribed to the lower t at x = 0.4, which will be illustrated in the following discussion. Moreover, it also implies that the limit of $(Mg_{1/3}Nb_{2/3})^{4+}$ substitution in Sr_2TiO_4 is less than 40% and further increase of x will lead to the appearance of Mg-/Nb-related secondary phases. Fig. 1(b) gives the enlarged XRD patterns of the present ceramics. With increasing x, the corresponding diffraction peaks shift gently towards the lower 2θ range, indicating a gradual expansion of unit cell. As shown in Fig. 1(c), with the substitution of larger $(Mg_{1/3}Nb_{2/3})^{4+}$ (0.667 Å) for Ti^{4+} (0.605 Å), both the cell parameters ascend monotonously with increasing x, and this further confirms that $(Mg_{1/3}Nb_{2/3})^{4+}$ has been successfully substituted into Sr_2TiO_4 ceramics. Moreover, a continuous decline of c/a value is also noticed (see Fig. 1(d)). This indicates that the preferred orientation along c axis is gradually suppressed with increasing x.

The SEM images of $Sr_2Ti_{1-x}(Mg_{1/3}Nb_{2/3})_xO_4$ ceramics are shown in Fig. 2. All the images demonstrate dense microstructures and an apparent evolution of grain morphology is observed. For $x \leq 0.2$, the grains generally exhibit long strip-like feature, and the columnar grains are gradually suppressed and then disappear with further increasing x. A similar result has also been reported in $(Sr_{1-x}Ca_x)SmAlO_4$ solid solutions [9] and the gradual decline of c/a value discussed above should be responsible for this phenomenon.

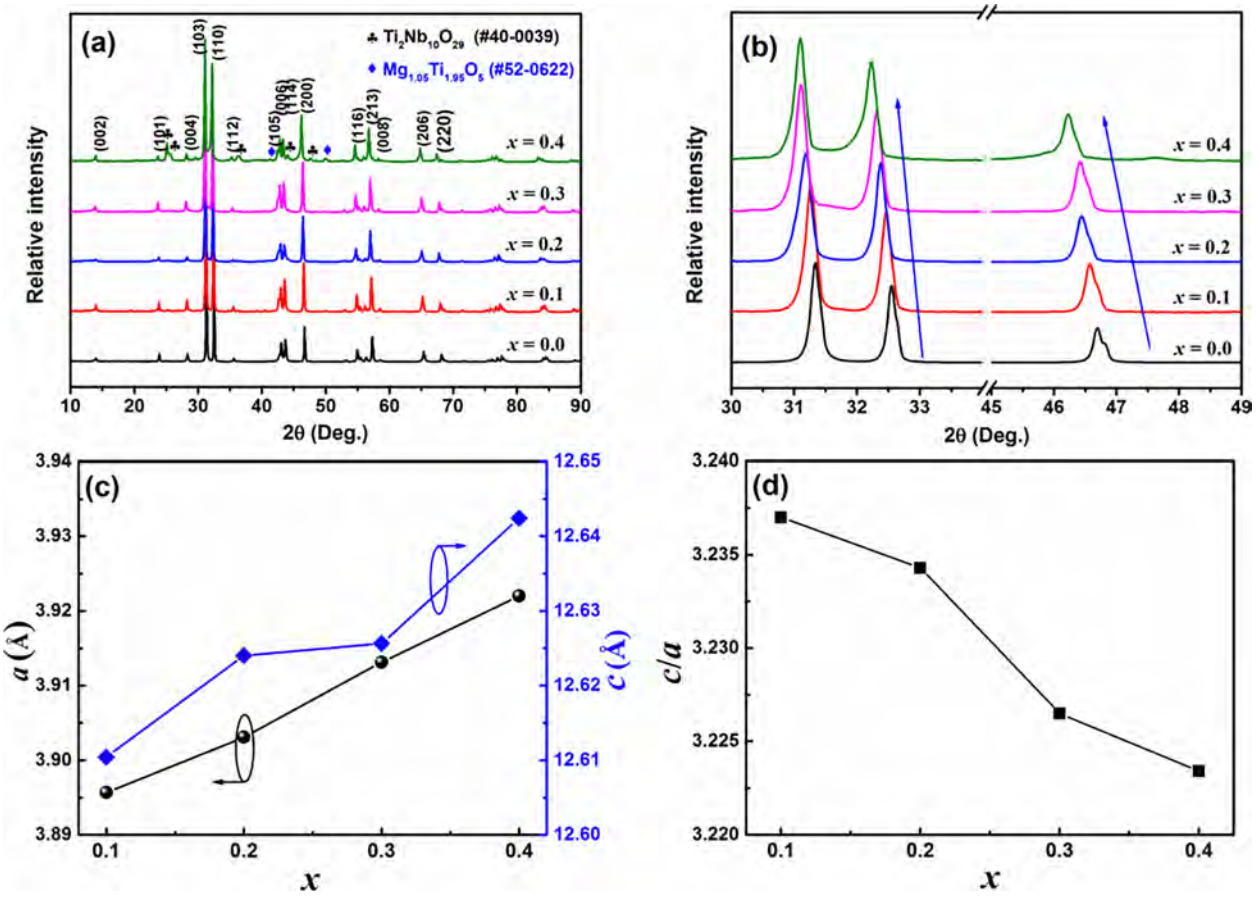

Fig. 1. (a) The XRD patterns of $Sr_2Ti_{1-x}(Mg_{1/3}Nb_{2/3})_xO_4$ ceramics. (b) Enlargement of the diffraction patterns in the 2θ range of 30–49°. (c, d) The lattice parameters (a, c) and c/a value as functions of composition x.

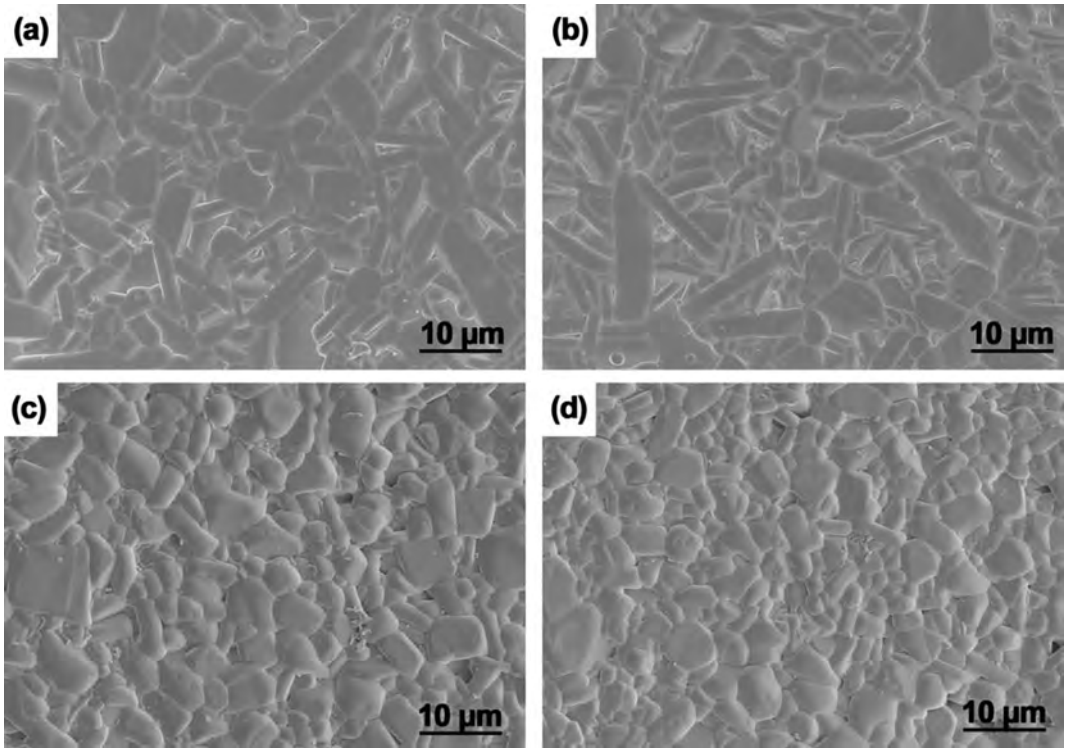

Fig. 2. The SEM images of $Sr_2Ti_{1-x}(Mg_{1/3}Nb_{2/3})_xO_4$ ceramics: (a) x = 0.1, (b) x = 0.2, (c) x = 0.3 and (d) x = 0.4.

The variation of ε_r and τ_f values of the present ceramics are plotted in Fig. 3(a). ε_r decreases monotonously from 42 at x = 0 to 26.3 at x = 0.4. It is notoriously known that the variation of ε_r should be mainly related to the ionic polarizability per volume. According to Shannon's additive rules [10], the theoretical ionic polarizability (α_{theo}) of $Sr_2Ti_{1-x}(Mg_{1/3}Nb_{2/3})_xO_4$ ceramics is calculated using the following equation, and the results are listed in Table 1.

$$a_{theo} = 2\alpha(Sr^{2+}) + (1-x)\alpha(Ti^{4+}) + x/3 \times \alpha(Mg^{2+}) + 2x/3 \times \alpha(Nb^{5+}) + 4\alpha(O^{2-}) \quad (1)$$

where, the ionic polarizability of Sr^{2+}, Ti^{4+}, Mg^{2+}, Nb^{5+} and O^{2-} are 4.24, 2.93, 1.32, 3.97 and 2.01 Å^3, respectively [10]. With increasing x, α_{theo} increases owing to the slight larger ionic polarizability of $(Mg_{1/3}Nb_{2/3})^{4+}$ (3.087 Å^3) than Ti^{4+} (2.93 Å^3). The different variation tendency of α_{theo} and ε_r should be ascribed to the expansion of cell volume, which might lead to a lower ionic polarizability per volume.

On the other hand, τ_f is related to the temperature coefficient of ε_r (τ_ε) and the linear thermal expansion coefficient (α_L) via the following equation [11]:

$$\tau_f = -\left(\frac{\tau_\varepsilon}{2} + \alpha_L\right) \quad (2)$$

where, for most ceramics, α_L is a constant value of ~10 ppm/°C. Therefore, the variation tendency of τ_f is mainly determined by τ_ε, which is closely related to ε_r. Consequently, τ_f indicates a similar changing trend with ε_r, and could be successfully tuned from 130 ppm/°C to 46.3 ppm/°C.

Fig. 3(b) shows the Qf value as functions of sintering temperature and x. For each composition, the Qf value increases with increasing sintering temperature until it reaches the maximum value at 1500 °C or 1525 °C, and then decreases with further increasing temperature. The optimum Qf value of each composition is plotted in Fig. 3(c). The Qf value exhibits an approximately linear decrease with increasing x, from 145,000 GHz at x = 0–51,000 GHz at x = 0.4. The decline of Qf with increasing x could be discussed from both intrinsic and extrinsic factors as the dielectric loss is sensitive to various parameters such as structural stability, phase compositions, etc. For the extrinsic part, the appearance of secondary phases at x = 0.4 should be the main reason for its abnormally low Qf value. While, for the intrinsic part, the tolerance factor has been widely adopted as a reliable empirical index in predicting the structural stability and an effective parameter in correlating the intrinsic structure with the Qf value. t is calculated from the effective ionic radius of each ions using the following expression [12].

$$t = \frac{r(Sr^{2+}) + r(O^{2-})}{\sqrt{2}[(1-x) \times r(Ti^{4+}) + x/3 \times r(Mg^{2+}) + 2x/3 \times r(Nb^{5+}) + r(O^{2-})]} \quad (3)$$

The calculated t as a function of x is plotted in Fig. 3(c). The evolution of t demonstrates a similar changing trend with Qf value, indicating that the decrease of t should be another major factor affecting the Qf value. The microwave dielectric properties of each composition are summarized in Table 1 and the optimal properties are achieved at x = 0.3 (ε_r = 28.5, Qf = 83,300 GHz, τ_f = 53 ppm/°C).

4. Conclusions

$Sr_2Ti_{1-x}(Mg_{1/3}Nb_{2/3})_xO_4$ ceramics were prepared via a standard solid state reaction method for the first time. XRD results reveal the formation of single-phased $Sr_2Ti_{1-x}(Mg_{1/3}Nb_{2/3})_xO_4$ solid solution in the range of $0 \le x \le 0.3$, and two kinds of secondary phases start to appear when x = 0.4. With increasing x, τ_f value can be successfully tuned towards zero and a good combination of microwave dielectric properties is obtained at x = 0.3 (ε_r = 28.5, Qf = 83,300 GHz, τ_f = 53 ppm/°C). This indicates that the substitution of $(Mg_{1/3}Nb_{2/3})^{4+}$ for Ti^{4+} is an effective way in adjusting the τ_f value of Sr_2TiO_4 ceramics and further modification of dielectric properties should be expected through suppressing the formation of impurities.

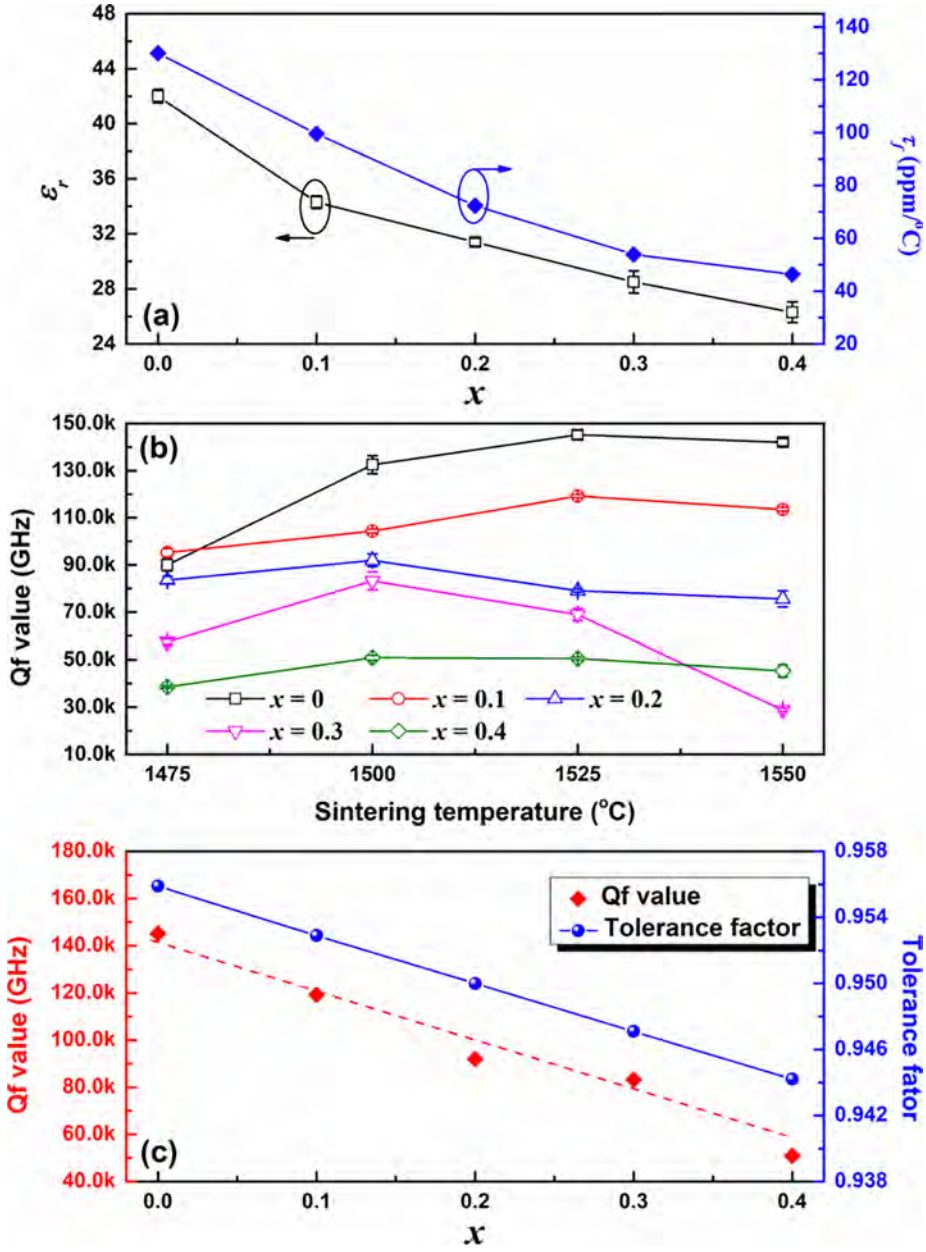

Fig. 3. (a) ε_r and τ_f values of $Sr_2Ti_{1-x}(Mg_{1/3}Nb_{2/3})_xO_4$ ceramics as a function of *x*. (b) *Qf* value of $Sr_2Ti_{1-x}(Mg_{1/3}Nb_{2/3})_xO_4$ ceramics as a function of *x* and sintering temperature. (c) Best *Qf* value of each composition as a function of *x*.

Table 1
The theoretical ionic polarizability, cell volume (V_m), relative density and microwave dielectric properties of $Sr_2Ti_{1-x}(Mg_{1/3}Nb_{2/3})_xO_4$ ceramics.

x	α_{theo} (Å^3)	V_m (Å^3)	Sintering Temperature (°C)	Relative Density	ε_r	*Qf* (GHz)	τ_f (ppm/°C)
0	19.450	190.076	1525	97.1%	42.0	145,000	130
0.1	19.465	191.379	1525	97.5%	34.3	119,000	99.5
0.2	19.480	192.316	1500	96.8%	31.4	92,000	72.3
0.3	19.495	193.329	1500	96.2%	28.5	83,300	53.0
0.4	19.510	194.468	1525	95.4%	26.3	51,000	46.3

Acknowledgement

The present study was financially supported by National Natural Science Foundation of China under grant number 51802062, 51701091 and 51672063.

Declaration of Competing Interest

We declare that we have no financial and personal relationships with other people or organizations that can inappropriately influence our work.

References

[1] K. Cheng, C. Li, H. Xiang, et al., Mater. Lett. 228 (2018) 96–99.
[2] C.H. Lee, N.D. Orloff, T. Birol, et al., Nature 502 (2013) 532–536.
[3] B. Liu, L. Li, X.Q. Liu, et al., J. Am. Ceram. Soc. 100 (2017) 496–500.
[4] C.W. Ahn, S. Nahm, S.J. Yoon, et al., Jpn. J. Appl. Phys. 42 (2003) 6964–6968.
[5] J.J. Bian, X.H. Zhang, J. Eur. Ceram. Soc. 38 (2018) 599–604.
[6] F. Zhao, Z. Yue, Y. Zhang, et al., J. Eur. Ceram. Soc. 25 (2005) 3347–3352.
[7] G.H. Chen, J.C. Di, H.R. Xu, et al., J. Am. Ceram. Soc. 95 (2012) 1394–1397.
[8] M.J. Pitcher, P. Mandal, M.S. Dyer, et al., Science 347 (2015) 420–424.
[9] M.M. Mao, X.M. Chen, Int. J. Appl. Ceram. Technol. 8 (2011) 1023–1030.
[10] R.D. Shannon, J. Appl. Phys. 73 (1993) 348–366.
[11] Z. Xu, L. Li, S. Yu, et al., Mater. Lett. 252 (2019) 191–193.
[12] V.M. Goldschmidt, Naturwissenschaften 14 (1926) 477–485.